EFFECT OF HETEROGENEITY AT THE FIBER/MATRIX SCALE ON PREDICTED FREE-EDGE STRESSES FOR A $[0/90]_S$ LAMINATED COMPOSITE

M. Keith Ballard[1] and John D. Whitcomb[2]

[1] Texas A&M University, Department of Aerospace Engineering kballard@tamu.edu
[2] Texas A&M University, Department of Aerospace Engineering, jdw@tamu.edu

Keywords: Fiber/matrix composites, Free-edge analysis, FEA, Microscale

ABSTRACT

The effect of the free-edge on the interlaminar stresses that develop in a $[0/90]_s$ laminated composite under uniaxial tension was explored while directly modeling the microstructure. A random arrangement of fibers was generated for each ply, and a large section of the laminate was modeled. The discrete case, where the fibers and matrix were directly modeled, was compared to the homogenous model, where plies were treated as homogeneous, transversely isotropic materials. The deformed cross-sections were compared for the two cases, showing that the discrete case exhibited local perturbations due to the heterogeneous microstructure. However, there was also a difference at a larger scale of up to 11% between the cases, indicating that the effective properties from a periodic analysis may be misrepresentative of the finite domain considered in this paper. The normal stresses along the ply interface were compared, showing great differences. The discrete case exhibited a complex pattern of stresses that depended on the fiber locations near the ply interface and the effect of the free-edge. In contrast, the homogeneous case predicted zero interlaminar normal stresses away from the free-edge and a stress singularity at the intersection of the free-edge and the ply interface. The effect of the fibers, which occurs without a free-edge present, and the free-edge effect were separated, showing that the fibers significantly affect the interlaminar normal stresses. Once isolated, the stresses that develop due to the free-edge effect matched well between the two cases, except very close to the free-edge, since the discrete case does not have a singularity on the ply interface. This initial study into the effect the heterogeneous microstructure on interlaminar stresses near a free-edge showed the importance of considering the discrete fibers near the interface if the interlaminar stresses are to be accurately predicted.

1 INTRODUCTION

Laminated composites exhibit many different types of failure modes, ranging from intra-ply cracking to delamination. The stresses near a free-edge are known to be critical and can induce free-edge delaminations, so it is important to understand the effect of the free-edge in order to accurately predict failure of laminated composites. For many years, researchers have used classical laminate theories, finite difference models, and finite element analysis (FEA) to characterize the effect of the free-edge for various types of layups with great success. [1] [2] [3] The models are used to determine apparent properties of laminates based on experiments, and effects of the layup and ply thickness have been studied thoroughly. However, researchers have almost always modeled the fiber/matrix plies as transversely isotropic, homogeneous materials because of the computational expense of modeling the fibers discretely and the relatively few FEA codes capable of distributed large-scale computing. Treating each ply as a homogenous, transversely isotropic material neglects the local effects of stiff fibers in a relatively soft matrix. Due to the much smaller scale of an individual fiber compared to that of a ply, the perturbation in the stress field due to actual heterogeneity will remain localized to a small region, but if the aim of an analysis is to predict when a ply crack or delamination will initiate, then local stress concentrations can be very significant. Consequently, some researchers have employed multiscale strategies to capture the effects of fibers in critical regions. [4] [5] In addition, some previous studies, including recent studies, have modeled discrete fibers near the free-edge, but relatively few fibers were considered due to the prohibitive computational challenges. [6] [7]

Computational power has continued to increase, making it possible to evaluate the accuracy of approximating a ply as a homogenous material by directly modeling the fibers within a much larger section of a composite laminate than done previously. This paper will model the fibers and matrix discretely for a section of a laminated composite under uniaxial tension, exploring the effect of discrete fibers on the stresses near and along the interface close to the free-edge. Due to restrictions of length for this paper, only the effect of discrete fibers on the resulting deformation and interlaminar normal stresses are considered.

This paper begins with a background section that describes the composite laminate and the smaller analysis region considered in this paper, the material properties used, and the finite element model. Next, the results are given, which is separated into three parts. First the deformed cross-sections are compared for the cases where fibers and matrix are modeled discretely and where plies are modeled as homogeneous materials. Second, the normal stresses along the ply interface are compared. Finally, the effect of fibers and the free-edge are separated for the discrete case to understand the contribution of each.

2 BACKGROUND

The following sections describe the composite laminate and the analysis region, the fiber and matrix properties and the homogenized properties for a lamina, and the finite element model.

2.1 Composite Laminate and Analysis Region

A $[0/90]_s$ cross-ply laminated composite under uniaxial tension was modeled to understand the stresses that develop near the free-edge between the 0^0 and 90^0 plies. This laminate was selected because it is the simplest laminate to exhibit free-edge stresses. The domain of an actual composite specimen is prohibitively large for discrete modeling of the fibers and matrix, but a much smaller unit cell can be considered that is representative of the entire specimen. Since the laminate is assumed to be symmetric about the planes z=0 and y=0, one quarter of the specimen can be considered. See Figure 1 for the coordinate system used. Along the x-axis, the y-z cross-section can be assumed to stay approximately planar during deformation, allowing a small slice along the x-axis to be modeled. Because of these approximations, the analysis region reduced to that shown in Figure 1a. The boundary conditions applied to the region are shown in Figure 1b. Any boundary conditions not explicitly shown in Figure 1b are zero-traction conditions. The applied displacement, U_0, is chosen such that the model experiences 1% strain in the x-direction. The dimensions of the region as labelled in Figure 1b are as follows: $L = 3.18e\text{-}4\ m$, $W = 5.77e\text{-}5\ m$, and $H = 1e\text{-}4\ m$. It should be noted that the fibers were, for the most part, randomly arranged in the matrix. This will be discussed further when the finite element meshes are discussed. Also, since almost free-edge analyses in the literature have used homogenized properties for each lamina, results using this approximation will also be presented for comparison.

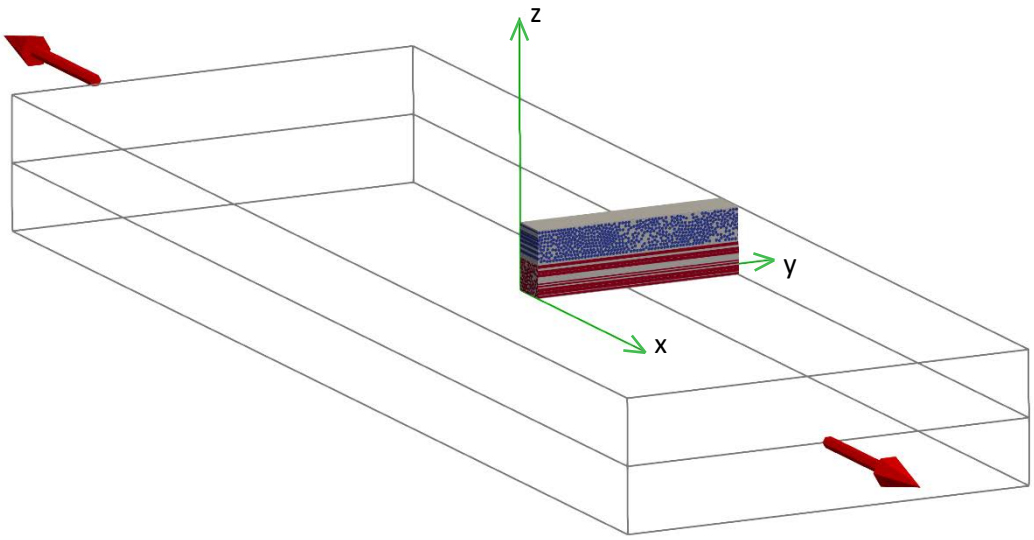

a) Laminated composite under uniaxial tension in direction of red arrows and the section discretely modeled

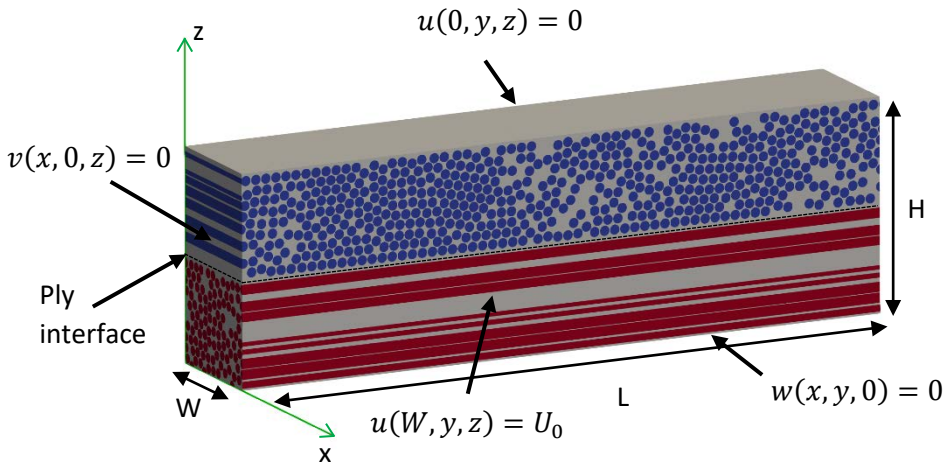

b) Boundary conditions for analysis region

Figure 1. Description of configuration

2.2 Material Properties

Two cases were considered in this paper. For the first case, the fiber and matrix were modeled discretely, which were assumed to be IM7 graphite fibers and 5220-4 epoxy matrix respectively. The properties for the epoxy matrix was taken from Ref. [8]. However, it was shown in Ref. [9] that the fiber properties need to be inversely determined using a consistent microstructure if the effective properties are to accurately represent the homogenized microstructure. In Ref. [9], the effective ply properties and matrix properties were taken from Ref. [8], and the apparent fiber properties were inversely determined. Those same apparent fiber properties determined in Ref. [9] were used in this paper to remain consistent between the discrete and homogenized cases. For the second case, effective properties were used for each ply, which were taken from [8], as mentioned before. For both cases, the materials were assumed to remain linearly elastic. Table 1 summaries the properties used for the fibers, matrix, and homogenized plies.

IM7 Graphite Fibers [9]	
E_1 (GPa)	276
E_2 (GPa)	26.0
G_{12} (GPa)	20.7
G_{23} (GPa)	7.55
ν_{12}	0.292

5220-4 Epoxy Matrix [8]	
E (GPa)	3.45
G (GPa)	1.278
ν	0.35

Effective IM7/5220-4 Lamina [8]	
E_1 (GPa)	165.5
E_2 (GPa)	10.34
G_{12} (GPa)	5.792
G_{23} (GPa)	3.315
ν_{12}	0.31
ν_{23}	0.56

Table 1: Material properties

2.3 Finite Element Model

This work used randomly generated fiber arrangements that were periodic in the plane of laminate to represent the cross-sections of each ply. The arrangements of fibers were created by randomly positioning fibers within the cross-sections and iteratively adjusting fiber positions to remove any spatial interference. The iterative algorithm used to remove overlap is described in Ref. [10]. A technique was described in Ref. [9] to create a minimum space between fibers, which involves a fictitious volume fraction Vf'. For this paper, a volume fraction, Vf, of 60% was assumed for each ply, while Vf' was specified to be 68%, resulting in fibers being at least 13% of a fiber radius away from another fiber. For the 0^0 ply, which has fibers aligned with the x-axis, the random arrangement was generated for the entire y-z cross section, which is shown in Figure 1b. For this cross-section, fibers were not allowed to cross the top and bottom boundaries normal to the z-axis during the generation of the random arrangement. For the 90^0 ply, which has fibers aligned with the y-axis, the random arrangement was generated for the x-z cross-section, while not allowing fibers to cross the top edge normal to the z-axis. However, the ply was assumed to be symmetric about $z = 0$, so fibers could either touch or cross exactly halfway to maintain a symmetry of the geometry. This is not completely realistic, since fibers can physically cross the mid-plane, resulting in no perfect symmetry about the mid-plane, but assuming that the laminate was symmetric about the mid-plane allowed half of the entire laminate thickness to be modeled. Once the geometry was created, a conforming quadratic triangle mesh was generated using a third-party library called Triangle. [11]

The cross-ply mesh was created by extruding the meshes of the cross-section of each ply in such a way to make it compatible with the other ply at the ply interface. It was assumed that the fibers are straight. The mesh for this paper contained about 14 million nodes or 42 million degrees of freedom (DoF), which requires the use of a finite element code capable of leveraging high-performance computing (HPC) systems. An in-house FEA code was used to perform the linear elastic analyses of this model, using the Texas A&M's supercomputing system called Ada. Data management was a significant challenge. A custom file-format was developed to store the required data for a distributed finite element analysis, and a ParaView reader plugin was developed to natively view the data. [12]

Almost all previous studies of free-edge stresses have assumed each lamina to be a homogeneous material with transversely isotropic material properties. For comparison purposes, the free-edge behavior for homogenized laminae was also calculated. The mesh used for the homogeneous case was made of 20-node hexahedral elements and contained about 240,000 nodes.

3 RESULTS

In this section, the results of the free-edge analysis with discrete fibers and matrix is compared to those of the homogenized model. The results can be separated into three primary sections. First the deformed cross-sections are compared. This is followed by a comparison of the normal interlaminar stresses. Finally, the effect of the discrete fibers and the free-edge are separated, providing an understanding of each and their contribution to the overall behavior.

3.1 Comparison of Deformed Cross-Sections

Figure 2a shows the deformed y-z cross-section at $x = 0$ for the discrete case, with an outline showing the deformed boundaries of the homogenized case. The deformed cross-sections in Figure 2 were exaggerated by 43x to clearly illustrate the differences, since the applied 1% strain results in small displacements. The displacement field was similar between the two models, though the largest displacement in the y-direction for the homogenized case was 11% less than that of the discrete fiber/matrix case and occurred at the top left corner of Figure 2a. This means the effective properties used for the homogenized case may not accurately representative of the heterogenous microstructure of the discrete case. However, it is important to remember that the fiber and matrix properties were chosen such that, for a periodic quasi-3D RVE, the effective response matches the effective laminar properties that were experimentally measured in Ref. [8]. However, each ply considered in this paper has a finite thickness. As a result, the 0^0 ply is only periodic along the x-axis, and the effective properties may not be as representative of this finite case as they are representative of the infinite periodic array considered in Ref. [9]. This discrepancy concerning using effective properties based on an infinite domain for an analysis of a finite domain contributes to the difference between the deformed cross-sections in Figure 2a. However, there is also the issue of the fiber volume fraction not being uniform within the 0^0 ply, which can be observed in Figure 2a. The non-uniform fiber volume fraction is also contributing to difference between the two displacement fields, but it is difficult to separate these two effects.

At the microscale, there were some notable differences between the two deformed shapes, but these differences are due to the perturbations caused by the discrete modeling of the heterogeneous microstructure. Along the top edge of Figure 2a, some of these perturbations can be observed, which are highlighted in Figure 2b.

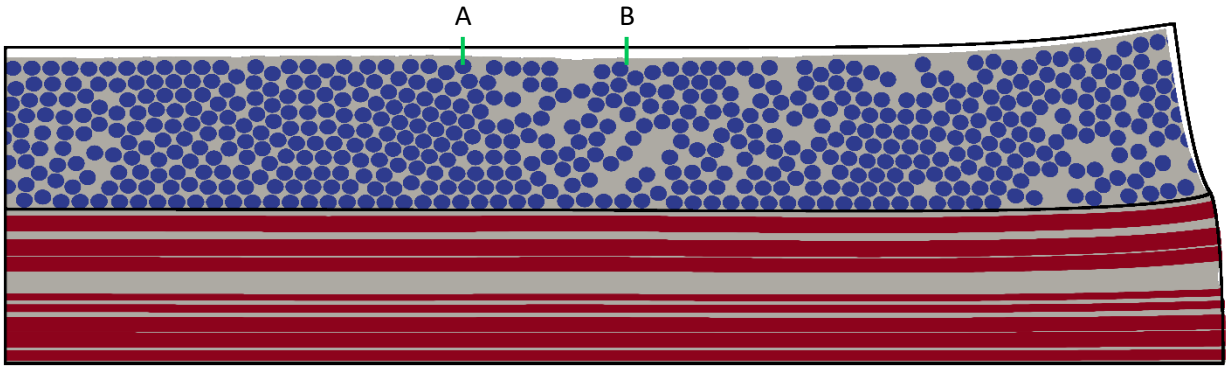

a) Deformed discrete fiber/matrix case with outline showing deformed homogenized case (43x displacement magnification)

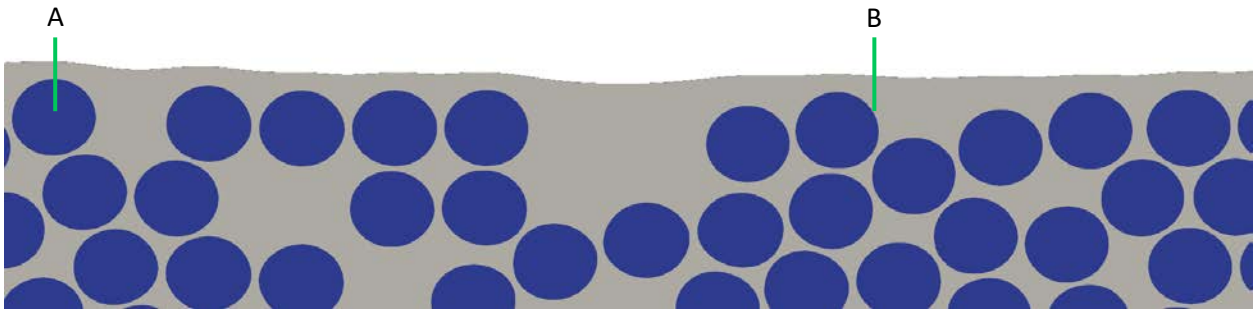

b) Deformed section along top edge in Figure 1a showing local perturbations

Figure 2. Deformed y-z cross-section at $x = 0$

3.2 Interlaminar Normal Stresses

The effect of the free-edge on the interlaminar stresses has been extensively studied using homogenized plies, but the effect of discretely modeling the fibers and matrix is explored in this paper. Figure 3 shows 3D surface plots to show the variation of the interlaminar normal stress σ_{zz} along the ply interface shown in Figure 1b. To the clarify the differences, the interface is displaced in the z-direction proportional to the magnitude of σ_{zz}.

Figure 3 reveals that the predicted interlaminar normal stresses are significantly different when the fibers and matrix are discretely modeled. The clearest difference is that the homogenized case predicts an ever-increasing normal stress near the free-edge, due to a singularity, while the discrete case predicts a much lower stress near the free-edge. In the homogenized case, a combination of the free-edge and material discontinuity at the ply interface creates a singularity, where $\sigma_{zz}\left(x, y, \frac{H}{2}\right) \rightarrow \infty$ as $y \rightarrow L$. However, in the discrete case, there is no such singularity at the ply interface, since there is only matrix material at the intersection of the free-edge and ply. Furthermore, the maximum stress for the discrete case does not occur at the free-edge, but rather about a fiber radius away from it.

For the discrete case, there are two mechanisms contributing to a very different stress distribution compared to the homogenized case. First, there is a local effect of the heterogeneous microstructure. The fiber locations relative to the interface and large mismatch of fiber and matrix properties for the discrete case create a non-zero σ_{zz} even far away from the free-edge. The effect of fibers on the interlaminar normal stress away from the free-edge can be seen near $y = 0$ in Figure 3, which is over 6 ply thicknesses away from the free-edge. By contrast, the homogenized case predicts that $\sigma_{zz}\left(x, y, \frac{H}{2}\right)$ goes to zero far away from the free-edge. Second, there is the effect of the free-edge that occurs at a larger scale than individual fibers and matrix. The free-edge still affects the interlaminar stresses, even if it no longer introduces a singularity for the discrete case. It is beneficial to separate these two factors to understand the importance of each, which is done in a later section. Based on Figure 3, it seems that the 90^0 fibers have a larger effect on the interlaminar normal stress than the 0^0 fibers, since the variation seen along any line parallel to the y-axis is significantly less than the variation of a line parallel to the x-axis. This claim will more thoroughly investigated in a later section when the effect of discrete fibers and the free-edge are separated.

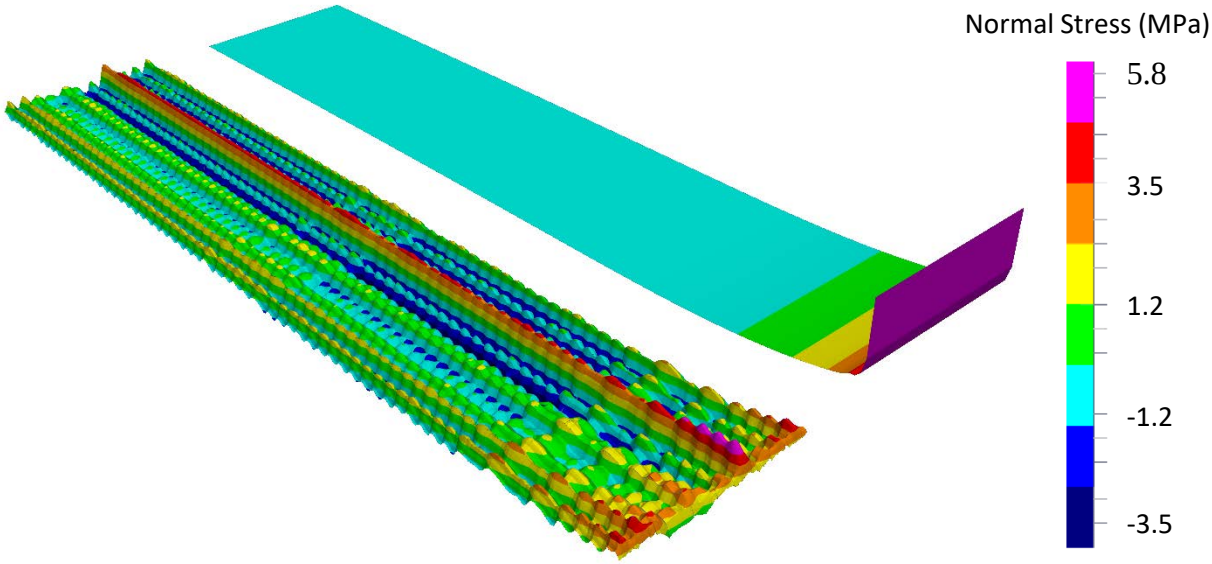

Figure 3. Comparison of σ_{zz} predictions (contours are based on color bar shown, and the surface is deformed proportional to the value of the normal stress)

Qualitatively, Figure 3 shows that the normal interlaminar stresses are very different between the two models, but it can be difficult to quantitively interpret the plots. To look at the differences more carefully, the interlaminar normal stress will be plotted from the free-edge to the mid-plane. For the homogeneous case, there is no variation along the x-direction, but since there is significant variation in the discrete fiber/matrix case, the distributions along four lines are shown.

Figure 4 shows the interlaminar normal stress as a function of the distance from the free-edge normalized by the ply thickness, which will be denoted d, for the two cases. The normalized distance from the free-edge is calculated by the equation below, where L and H are dimensions of the model shown in Figure 1b.

$$d = \frac{2(L - y)}{H} \tag{1}$$

The homogenized case exhibits the singularity at the free-edge as mentioned earlier. The general trend is a sharp decrease in σ_{zz} for about 1 ply thickness from the free-edge and then increases to approach 0. For all four positions considered for the discrete fiber/matrix case, the stress generally tends to decrease until about 1 ply thickness from the free-edge, but there are also significant oscillations. The fiber positions and distance from the ply interface are plotted in Figure 5 using red circles. It appears that most of the troughs of the oscillations lie very close to a 0^0 fiber near the ply interface. Furthermore, paths 1 and 2 had similar stresses, and paths 3 and 4 had similar stresses. But there is a large difference in interlaminar normal stresses between the two pairs of lines. This seems to be correlated to the positions of the 90^0 fibers. An important difference in the discrete and homogenized models occurs right at the free-edge. The homogenized case exhibits a singularity, while the discrete case decreases locally to a finite value, since there is no material discontinuity at the ply interface.

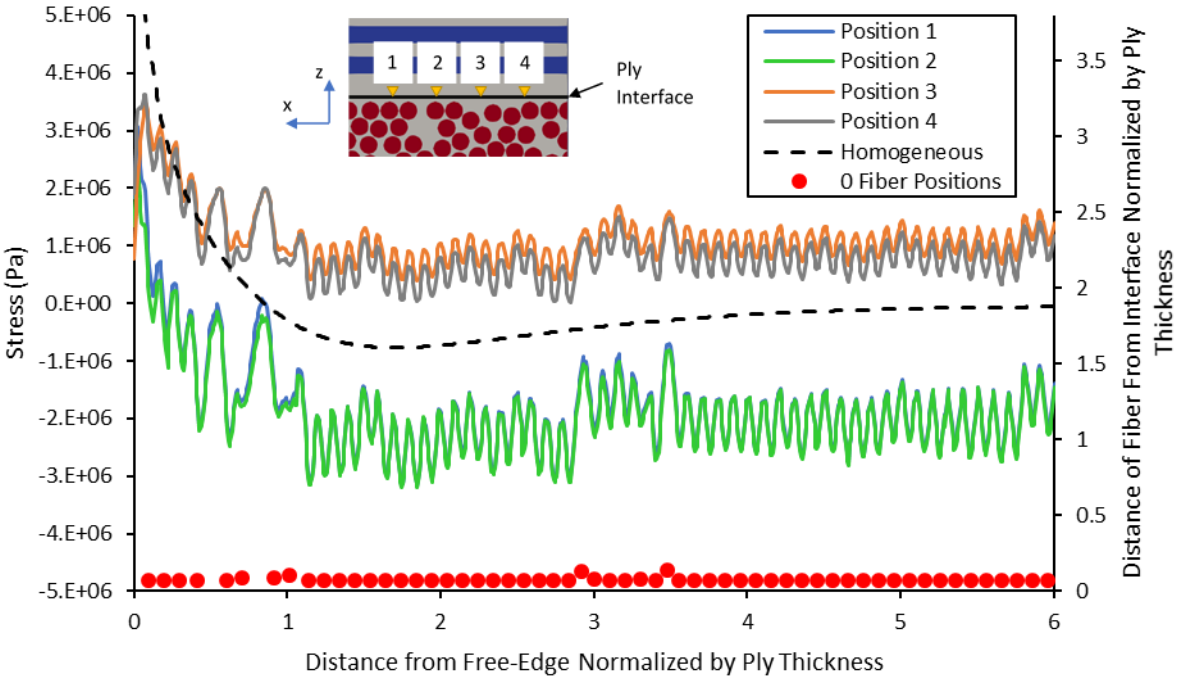

Figure 4. Interlaminar normal stress plotted along lines parallel to the y-axis versus the distance from the free-edge normalized by the ply thickness. The 0^0 fiber positions are also shown.

3.3 Separation of the Effect of the Free-Edge and Discrete Fibers

As discussed before, there are two effects contributing to the contours shown in Figure 3 for the discrete case. First, the presence of free-edge will perturb the stresses of the material close to it. Second, the interactions of 0^0 and 90^0 fibers near the ply interface will cause perturbations of the stresses, even if the material is away from the free-edge. To isolate the effect of the free-edge, the predicted stresses in the material if it was away from the free-edge is needed. To do this, an assumption is made that more than three ply thicknesses away from the free-edge is far enough away for the free-edge to have a minimal effect on the stress distribution compared to the effect of the fiber positions. With this assumption, another set of boundary conditions was applied to the exact same discrete model shown up to this point. Instead of the positive y-face being the free-edge, the negative y-face will be free, and the positive face will become a plane of symmetry. The stresses within three ply thicknesses of the $y = L$ will be assumed to be minimally affected by the free-edge, leaving the effect of the discrete fibers.

Figure 5 shows the normal stresses along the ply interface for the material close to the positive y-face ($y = L$) if it was far away from the free-edge. Positions 1 and 2 are very close to 90^0 fibers that lie near the ply interface. Furthermore, the troughs of the stress oscillations closely align with 0^0 fiber positions. Considering this when interpreting Figure 5, it is concluded that when fibers in both plies lie close to each other, a compressive stress state is formed. This is a similar trend to one observed in 2D fiber/matrix analyses of random RVEs. McLendon et. al. observed that compressive stresses form when fibers come close together in a uniaxial lamina under tension. [10] Similarly, a compressive effect is caused by fibers being close on each side of the ply interface, when the laminate is subjected to a tensile load. This behavior is important to consider if the strength of laminates near critical areas, such as a free-edge, is to be optimized.

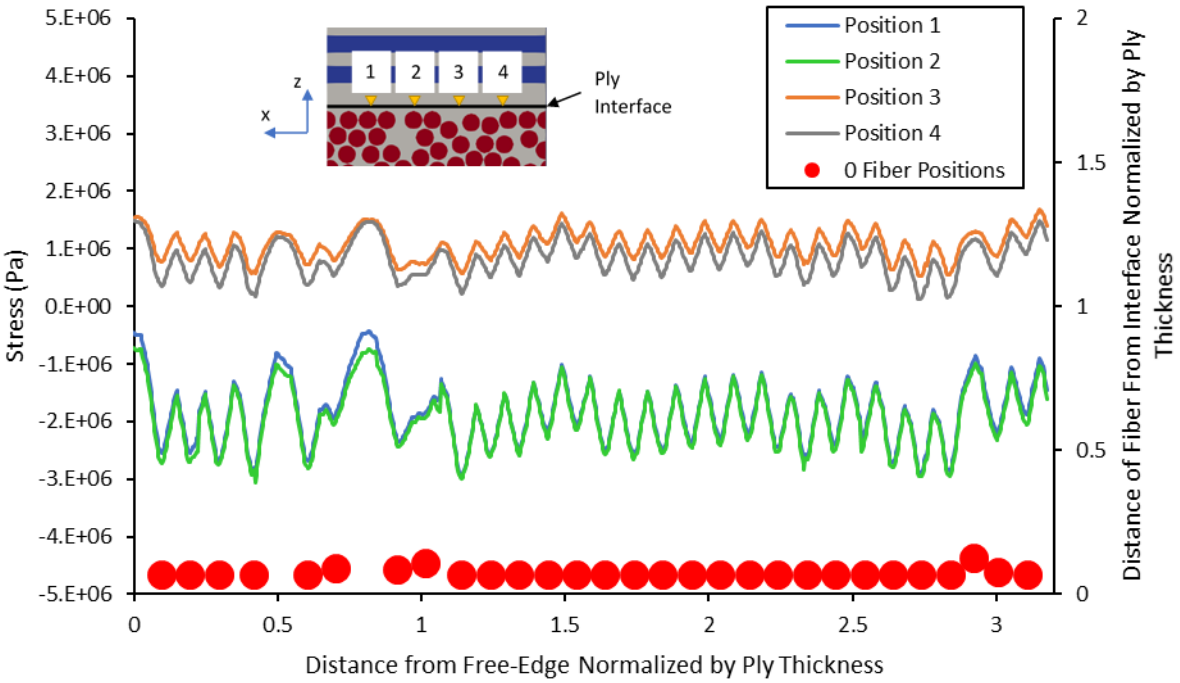

Figure 5. Interlaminar normal stress for the material within three ply thickness of the positive y-face of the model if the material was away from the free-edge (0^0 fiber positions are also shown)

Since linear elasticity is assumed in this paper, superposition can be used, and the stresses shown in Figure 5 can be subtracted from the stresses near the free-edge shown in Figure 4 to isolate the effect of the free-edge. Figure 6 shows the stresses induced by the free-edge effect along the ply interface, as well as 0^0 fiber positions and the stresses near the free-edge for the homogenous case.

After the free-edge effect was isolated, the stress distribution for the discrete case matches the homogenous case much better than was shown in Figure 4, which did not isolate the free-edge effect. There is still a significant difference very close to the free-edge since the stress singularity does not exist for the discrete case, but after about 10% of a ply thickness away from the free-edge, the stress distributions are quite similar. There are still oscillations indicating that the 0^0 fibers near the interface affect the stresses induced by the free-edge. However, there is very little difference between the four paths considered. This means that the free-edge effect is insensitive to the 90^0 fibers near the ply interface. This is a different behavior than the effect of the fibers near the interface shown in Figure 5, which showed that the 90^0 fibers had a significant effect.

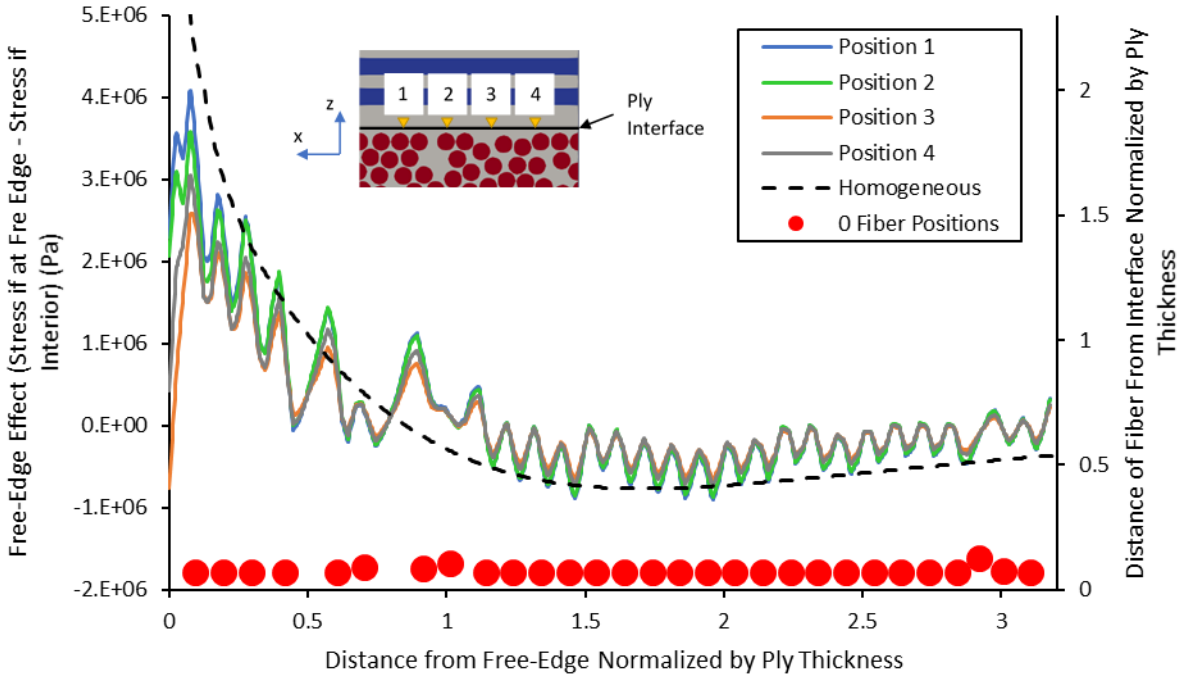

Figure 6. Predicted variation of σ_{zz} due to just the free-edge effect (0^0 fiber positions are also shown)

4 CONCLUSIONS

For a $[0/90]_s$ laminated composite, fibers near the interface, especially the 90^0 fibers, have a significant effect on the stress state along the ply interface. This is the case whether the material is near the free-edge or well within the interior of the specimen. For this configuration, the fibers near the interface perturbed the stresses by up to 75% of what the free-edge perturbed the stresses, indicating that the effect cannot be ignored for this laminate. However, this initial study considered a $[0/90]_s$ cross-ply laminate for its simplicity, but this layup is seldom used in engineering applications. Other types of layups have been known to exhibit a stronger free-edge effect than this case, so future work is needed to understand how the heterogeneous microstructure affects interlaminar stresses for other types of laminates.

ACKNOWLEDGEMENTS

This work was supported by the Department of Defense (DoD) through the National Defense Science & Engineering Graduate Fellowship (NDSEG) Program. In addition, the authors acknowledge the Texas A&M Supercomputing Facility (http://sc.tamu.edu/) for providing computing resources used in conducting the research reported in this paper.

REFERENCES

[1] N. J. Pagano, Free edge stress fields in composite laminates, *International Journal of Solids and Structures*, **14**, 1978, pp. 401-406.

[2] I. S. Raju, J. D. Whitcomb and J. G. Goree, A new look at numerical analyses of free-edge stresses in composite laminates, 1980.

[3] J. D. Whitcomb, I. S. Raju and J. G. Goree, Reliability of the finite element method for calculating free edge stresses in composite laminates, *Computers & Structures*, **15**, 1, 1982, pp. 23-37.

[4] F. Feyel and J.-L. Chaboche, FE^2 multiscale approach for modelling the elastoviscoplastic behaviour of long ®bre SiC/Ti composite materials, *Comput. Methods Appl. Mech. Engrg.*, **183**, 2000, pp. 309-330.

[5] A. Nosier and M. Maleki, Free-edge stresses in general composite laminates, *International Journal of Mechanical Sciences*, **50**, 2008, pp. 1435-1447.

[6] S. Chung, Effects of Interlaminar Stress Gradients on Free Edge Delamination in Composite Laminates, Drexel University, 2003.

[7] N. Rajender, V. Rajasekhar and K. Vijay, Micromechanical Modeling of Fiber/Epoxy Unidirectional Laminates Using FEA, *The International Journal Of Engineering And Science*, **4**, 9, 2015, pp. 54-75.

[8] N. J. Pagano, G. A. Schoeppner and R. Kim, Steady-state cracking and edge effects in thermo-mechanical transverse cracking of cross-ply laminates, *Composite Science and Technology*, **58**, 1998, pp. 1811-1825.

[9] M. K. Ballard, W. R. McLendon and J. D. Whitcomb, The influence of microstructure randomness on prediction of fiber properties in composites, *Journal of Composite Materials*, **48**, 29, 2014, pp. 3605-3620.

[10] W. R. McLendon and J. D. Whitcomb, Micro-scale analysis for the prediction of strength under biaxial thermomechanical load, *Proceedings of the American Society for Composites*, 2012.

[11] J. Shewchuck, Triangle: Engineering a 2D quality mesh generator and Delaunay triangulator, *Applied Computational Geometry*, **1148**, 1996, pp. 203-222.

[12] A. Henderson, ParaView guide, a parallel visualization applicaiton, Kitware Inc., 2007.

[13] H. Y. Sarvestani and M. Y. Sarvestani, Free-edge stress analysis of general composite laminates under extension, torsion and bending, *Applied Matematical Modelling*, **36**, 2012, pp. 1570-1588.

[14] J. D. Whitcomb and I. S. Raju, Superposition method for analysis of free-edge stresses, *Journal of Composite Materials*, **17**, 1983, pp. 492-507.